Chronological Persistence of *Acropora cervicornis* at Coral Gardens, Belize

By Tanner Waggoner

Advisor: Dr. Lisa Greer

Washington and Lee University Department of Geology

Lexington, Virginia 24450

Table of Contents

Abstract

Acropora cervicornis (staghorn coral) is an important framework-building scleractinian coral that dominated many Caribbean reefs throughout the Pleistocene and Holocene. *Acropora* spp. suffered collapse throughout the Caribbean since the 1980s as a result of white band disease and other stressors. Despite widespread decline, large populations of *Acropora* spp. are currently thriving at Coral Gardens Reef, Belize, south of Ambergris Caye where live coral cover is as high as 50% in some areas. This project aims to discern whether these populations were established after the Caribbean acroporid collapse or whether they are remnant populations from before the 1980s. To determine the timing of *Acropora* spp. dominance at Coral Gardens, pristine aragonite material was sampled from dead coral skeletons excavated from stratigraphic 'pits' in the coral death assemblage at three underwater sites. Of the three sites, Pits A, B, and C extended approximately 1 meter, 1.2 meters and 2 meters beneath the reef surface, respectively. Six aragonite samples were extracted from Pit A, 17 from Pit B, and 16 from Pit C, and aged using conventional radiocarbon dating techniques. Carbon isotope ratios from radiocarbon analysis for samples from the dead assemblage indicate that *A. cervicornis* growth was initiated prior to the well-documented spike in atmospheric radiocarbon caused by nuclear weapons testing (late 1950s) and persisted throughout the mid-1960s. However, due to the lack of high resolution post-bomb radiocarbon calibration data for marine reservoir effects near Belize, additional dating techniques were needed to resolve the age of the more recent *A. cervicornis* corals. We used high-precision U-Th dating recently developed by Clark et al. (2014a) to better constrain the chronological persistence of *A. cervicornis* at Coral Gardens. ^{230}Th age data suggest that some of the *A. cervicornis* populations in Coral Gardens survived the wide-spread 1980s Caribbean acroporid coral collapse and that corals from beneath

the living *A. cervicornis* canopy are synchronous with those taken from the surface of Pit C. Results suggest some degree of continuity in reef growth at this site amidst greater Caribbean collapse of *Acropora* spp.

Introduction

Background

It is widely accepted that *A. cervicornis* was a dominant coral component of Caribbean reefs throughout the Pleistocene and Holocene (e.g.: Jackson, 1992; Greenstein et al., 1998; Wapnick et al., 2004; Pandolfi and Jackson, 2006; Greer at al., 2009). Few sites in the Caribbean exhibit well-preserved, sub-aerial records of *A. cervicornis* in limestone fossils due to rising sea levels in the post-glacial Holocene (Greer et al., 2009). However, data from well-exposed reef crests (e.g.: Burke et al., 1977; Macintyre et al., 1977; Jackson, 1992) provide a wealth of information about the persistence of *A. cervicornis* through the Holocene and Pleistocene. Using core data from Belizian reefs, Aronson and Precht (2001) suggest that prior to the 1980s *A. cervicornis* was a primary geological component to Belizean reefs for the past three millennia. At numerous sites in the Caribbean, including Florida (Shinn, 2003), Mexico (MacIntyre et al., 1977), the Bahamas (Newell and Rigby, 1957), Barbados (Mesolella, 1967), Jamaica (Goreau and Goreau, 1973), and the Dominican Republic (Greer et al., 2009), fossilized reefs from the Holocene are tributes to the impressive reef building capacity of *A. cervicornis* (Mesolella, 1967; Goreau and Goreau, 1973; Jackson, 1992; Johnson et al., 1995; Macintyre et al., 1977). *A. cervicornis* is the fastest growing coral in the Caribbean, making it one of the most important primary reef builders (NOAA 2014).With its interconnected morphology of durable calcium carbonate branches, *A. cervicornis* grows into complex frameworks that provide protection and habitat for a variety of benthic organisms (Fig. 17) (Miller et al., 2002; NOAA 2014). *A.*

cervicornis typically inhabited intermediate depths varying from 2-25 meters. Precise depths were strongly influenced by wave action and depended on if populations inhabited either protected fore-reef, back-reef, or lagoonal habitats (e.g.: Hubbard, 1988; Adey, 1978; Aronson and Precht, 2001; Bruckner, 2003).

Despite dominating Caribbean reefs in the Pleistocene and Holocene, *A. cervicornis* has declined substantially in the modern (e.g.: Gardner et al., 2003). Studies propose that Caribbean *A. cervicornis* declined over 90% in the past four decades in response to anthropogenic and natural disturbances (e.g.: Aronson and Precht, 2001; Miller et al., 2002; Bruckner, 2003; Wapnick, 2004; Pandolfi and Jackson, 2006; Vollmer and Palumbi, 2007; Greer et al., 2009; NOAA 2014). Other studies offer an alternative theory, suggesting that *A. cervicornis* was declining prior to the 1980s and throughout the 20th century (Jackson et al., 2001, Pandolfi et al., 2003; Cramer et al, 2012). Acknowledging that the former theory is most widely accepted, researchers have debated whether the 1980s acroporid die-off was unique or preceded by significant mortality events of comparable magnitude (e.g.: Aronson and Precht, 2001; Aronson et al., 2002; Shinn et al., 2003; Greer et al., 2009; Cramer et al., 2012). With varying accounts of A. *cervicornis* persistence in the fossil record (e.g.: Greenstein et al., 1998; Aronson and Precht, 2001; Aronson et al., 2002; Shin, 2003; Greer et al., 2009), it is near impossible to conclude that the 1980s Caribbean regional die-off is unprecedented. For example, Shinn et al. (2003) makes note of a 500-year hiatus in growth of *A. cervicornis* on Florida Reefs that occurred approximately 4,500 years ago. On the other hand, fossilized *A. cervicornis* in reef cores sampled from Belize by Aronson and Precht (2001) display no sign of any regional hiatus during the Pleistocene and Holocene. Additionally, Greer et al. (2009) suggests that growth of *A. cervicornis* has been nearly continuous the for at least a 2,000 year period from the middle to

early Holocene. Whether or not the recent die-off of *A. cervicornis* is anomalous, many studies do agree about the disturbances that caused recent decline. While overfishing and hurricanes have contributed, the majority of the 1980s regional decline in Caribbean acroporids can be attributed to white-band disease (e.g.: Aronson and Precht, 2001; Bruckner, 2003; Vollmer and Kline, 2008; Kline and Vollmer, 2011).

White-band disease (WBD) was first recognized in the late 1970s as the outcome of a bacterial pathogen (Kline and Vollmer, 2011) that inflicts severe damage on *A. cervicornis* and *A. palmata* (Gladfelter 1982; Aronson and Precht, 2001) Recently, Randall and Woesik (2015) suggested that the recent onset of WBD is linked to rising ocean surface temperatures. This information coupled with knowledge of human-induced climate change (e.g.: Rosenzwieg et al., 2008) raises question about the impact of anthropogenic activity on the health of *A. cervicornis*. Prior to the 20th century and throughout the Holocene, a variety of disturbances such as hurricanes (Woodley, 1989; Rogers 1993; Aronson and Precht, 2001), coral predators (Lessios, 1988; Knowlton et al., 1990), cold water stress (Porter et al., 1982) and thermally-induced bleaching (Glynn, 1993) have plagued the existence of *A. cervicornis* across the Caribbean. But even during periods of deglaciation and intense sea-level fluctuation, *A. cervicornis* kept pace with changing sea levels (Aronson and Precht, 2001; Greer et al., 2009). And despite these natural disturbances, *A. cervicornis* continued to thrive in the Caribbean (Aronson and Precht, 2001). While evidence may suggest that anthropogenic activity may be related to the onset of WBD, this idea is still widely debated and no definitive conclusion can be made. More quantitative data regarding the persistence of *A. cervicornis* is needed to settle such disputes.

One step towards better understanding vulnerability of *A. cervicornis* is to study living examples that persisted through the 1980s Caribbean die-off. Once such populations have been confirmed, ambient conditions at the host location could then be widely studied and quantified to determine what strengthened the likelihood of survival. Significant populations of living *A. cervicornis* have been documented at few locations in the Caribbean (Aronson and Precht, 2001), including the Dominican Republic (Lirman et al., 2010), Honduras (Keck et al., 2005; Purkis et al., 2006), Mexico (Larson et al., 2014), Florida (Vargas-Angel et al., 2003; Lidz and Zawada, 2013), and Coral Gardens, Belize (Greer et al., 2015; Busch et al., *in press*). Attempts have been made to characterize the current spatial distribution of *A. cervicornis* at these sites (e.g.: Purkis et al., 2006; Busch et al., *in press*; Huntington and Miller, 2014), but these studies simply characterize a snapshot in time of *A. cervicornis* health. Without high-resolution, quantitative data on a temporal scale for modern *A. cervicornis* reefs, we cannot determine how modern populations of healthy *A. cervicornis* relate to the 1980s die-off.

Quantitative data regarding the persistence of *A. cervicornis* reefs prior to the 1980s and extending through the recent die-off is rare (Miller et al., 2002; Cramer et al., 2012). One of the exceptions being a study where Cramer et al. (2012) used radiocarbon dating and fluctuations in biostratigraphy to study the persistence of *A. cervicornis* on a reef near Bocas del Toro, Panama for four prior centuries into the modern. Results from their study contradict the most commonly accepted theory that the health of *A. cervicornis* on Caribbean reefs declined suddenly in recent decades due to the onset of WBD (e.g.: Aronson and Precht, 2001; Aronson et al., 2005). However, Cramer's (et al., 2012) investigation certainly exemplifies the importance of quantitative data and how it can be used to confirm or deny qualitative accounts about the persistence *A. cervicornis*.

Our study aims to determine whether living *A. cervicornis* at Coral Gardens persisted through or recovered after the 1980s die-off using newly-developed, high-precision U-Th dating and conventional radiocarbon (^{14}C) dating. If *A. cervicornis* persisted through the 1980s die-off, then we suggest that Coral Gardens is a legitimate ecological refugia. Data was first published on Coral Gardens in 2015 by Greer et al. (2015) and Busch et al., (*in press)* and these studies are firsts of their kind to examine the persistence of modern *A. cervicornis* populations at Coral Gardens.

Radiocarbon Dating Background

Carbon isotope ratios in the atmosphere and oceans vary significantly due to a temporal delay in equalization and irregular oceanic mixing currents (Manz, 2015). For this reason, a 'global marine reservoir correction' is applied to more accurately date marine organics with radiocarbon analysis (Stuiver et al., 1986; Reimer et al., 2013; Manz, 2015). However, carbon isotope ratios can vary significantly on a spatial scale (Ulm, 2006). Additional regional corrections from the global marine averages in carbon isotope ratios can increase accuracy of aging marine carbonates with radiocarbon analysis (Ulm, 2006). In relation to this study, radiocarbon analysis for dating purposes has been widely used for marine carbonates in the Caribbean (e.g.: Macintyre et al., 1977; Aronson and Precht, 2001; Greer et al., 2009; Cramer et al., 2012). However, the closest available carbon isotope data to Coral Gardens was published by Ellen Druffel (1981), who took radiocarbon measurements of a coral core of known age from Glover Reef, Belize. Druffel (1981) built a valuable, dataset of carbon isotope ratios unique to the region. This marine, regionally corrected dataset is proximally the nearest available to Coral Gardens identified in scientific literature. However, the dataset created from radiocarbon analysis of corals at Glover Reef is only applicable to carbonate samples 1868-1977 in age (Fig. 8),

leading us to explore high-precision U-Th dating for aging modern carbonates (Clark et al., 2014a).

Study Site

Coral Gardens [17° 49’ 54.7644”, 87° 59’ 29.9743”], located approximately 6 kilometers South East of Ambergris Caye, Belize, is situated inshore of the Mesoamerican barrier reef (Fig. 13). This shallow, lagoonal patch reef is dominated by scleractinian acroporid corals (Irwin et al., *in review;* Busch et al., *in press*) with beds of seagrass and coarse-grained sediment scattered between reefs (Fig. 14). Massive thickets of *A. cervicornis* cover approximately 7.5 acres, making coral Gardens one of the largest recorded discoveries of this species in the Caribbean (Fig. 17) (Busch et al., *in press*). In 2011 Greer et al. (2015) surveyed the area and established 5 semi-permanent transects over separate canopies of *A. cervicornis* with the most prolific growth to be compared with data gathered in subsequent years (Fig. 14). In 2014, Busch et al. (*in press*) mapped live coral cover for 37 m^2 quadrants at Coral Gardens, discovering an average of 29.85% living coral cover (Greer et al., 2015). A subset of the population, Transect 5 (T5), is of particular interest with an average live coral cover per m^2 quadrant of 50.27% (Fig. 14; Fig. 17) (Greer et al., 2015*;* Busch et al., *in press*). In addition to the thriving *A. cervicornis* thickets at Coral Gardens (Fig. 17) is a vast area of algal and coral encrusted dead *A. cervicornis* reef framework (Fig. 18). Three pits were dug over two years through dead, crusted *A. cervicornis* at the surface and loosely-situated fragments in the subsurface. (Pits A, B, and C – Fig 14). Pits A and B were dug in 2014 in an attempt to determine the age of coral at the bottom of stratigraphic sections using conventional radiocarbon dating. Pit C, the nearest pit to the modern canopy at Transet 5, was dug in 2015 to construct a chronological record of *A. cervicornis* in the uppermost section using a combination of conventional radiocarbon and a newly-developed high-precision

U-Th dating techniques (this study; Clark et al., 2014a). The former of the two dating techniques requires a calibration curve complete with a regional offset from the global average in marine radiogenic carbon (Reimer et al., 2013). However, regionally corrected radiocarbon data for this region exists for dates only prior to 1977 in the modern (Druffel, 1981), forcing us to explore alternative dating techniques. We utilized a newly developed, high-precision ^{234}U-^{230}Th dating to determine the ages of modern coral samples at Coral Gardens (Clark et al., 2014a).

Methods

Sample Collection and Preparation

Using a hammer and chisel we dug three separate pits, each approximately 1 meter wide through consolidated rubble of dead *A. cervicornis* at Coral Gardens (Pit C – Fig. 12). *A. cervicornis* fragments were extracted approximately every 5 cm in stratigraphic order at each site. Samples taken from near the reef-surface were heavily bored and crusted from years of exposure to biological activity and were overgrown with vast amounts of attached foraminifera and fleshy algae (Fig. 15). Towards the base of the dead sections, coral samples were encrusted with coralline algae, yet were less porous than those near the top due to lack of prolonged exposure to weathering at the reef surface.

Excavations of all three pits were completed by divers using SCUBA (Fig. 11). Pits A and B were dug in 2014 and were approximately 1 meters and 1.2 meters deep beneath the surface of the reef, respectively. Pit C was dug in 2015 and was approximately 2 meters deep (Fig. 12), yielding over 110 samples alone during excavation. Pit locations varied significantly and were chosen in relation to thriving populations of *A. cervicornis* in the area (Fig. 14). Transect 5, a semi-permanent study-site established in 2014 is projected above the most successful modern canopy of *A. cervicornis* (Fig. 14; Fig. 17) Live coral cover at Transect 5 was

an average of 50.27% (Greer et al., 2015; Busch et al., *in press*) when surveyed in 2014. In 2015, dead *A. cervicornis* fragments were retrieved from beneath entangled *A. cervicornis* branches at Transect 5. Using an extendable tool, we reached through and beneath the modern canopy to extract pieces of loosely situated *A. cervicornis* at several locations around coral thickets at Transect 5. One recently bleached sample was extracted from the tip of a coral branch for calibration purposes.

In the field, samples were cleaned of organic matter using a chemical solution of 50% bleach by volume. Upon returning to Washington and Lee University in Lexington, VA, corals were cleaned more extensively as outlined below. Non-aragonite material was first removed from each coral fragment using a tile saw (MK Diamond Products Model 151881 – BD). Outer edges in the longitudinal direction of each coral fragment were carefully shaved-off to remove fleshy algae, coralline algae, and foraminifera that had encrusted to the surface (Fig. 9; Fig.10). Substantial amounts of material were removed from the near-surface samples using the carbonate rock saw because aragonite quality had been compromised by bioturbation.

Samples were analyzed beneath an X-Ray Diffraction Analyzer (XRD) (DIANO 2100E) and Scanning Electron Microscope (SEM) (ZEISS MODEL: EVO MA15) for sample quality control. Subsamples were powdered using a mortar and pestle and fixed to glass slides by saturating it with rubbing alcohol and allowing time to dry. The XRD was used to verify that crystal structure of the samples were indicative of aragonite contents and not calcite (Fig. 1). Under the SEM, high-resolution images were interpreted to further verify sample quality and identify impurities (Fig. 2). Aragonite samples containing visible calcite crystals or organic impurities were discarded (Fig. 3).

In addition to verifying sample quality, we gathered stable carbon and oxygen isotope data using a Mass Spectrometer (Model: Thermo Scientific Stable Isotope Ratio) benchtop at Washington and Lee University for ^{14}C calibration purposes. Third subsamples were powdered from each primary sample with a mortar and pestle for mass spectrometry analysis following a procedure outlined below from Yates et al., (*thesis*). Approximately 0.5 grams were weighed using a high-resolution scale (Sartorius) and vacuum sealed in a glass tube. These tubes were held static in the GC Pal Autosampler at 21℃. Helium air that was injected inside the tubes using the Finnigan GasBench II to flush the samples. Once flushing was complete, .02 mL of Sigma-Aldrich 99.0% pure H_3PO_4 was injected directly onto powdered samples through permeable seals of the tubes. Each powdered sample reacted with H_3PO_4 for one hour to generate CO_2. Prior to analysis, samples underwent a Zero Enrichment Test to ensure accurate results from the mass spectrometer. Using the gas bench, powdered samples were fed to the mass spectrometer and analyzed. $\delta^{18}O$ and $\delta^{13}C$ ratios (‰) were calculated in relation to SMOW and VPDB standards, respectively.

Radiocarbon Dating and Correction

One cm^3 each of pure aragonite was subsampled from sixty-five primary samples for radiocarbon analyses. Samples were crushed to approximately 2mm-sized fragments using a hammer. From these larger samples, ten (10) milligrams of the cleanest fragments were placed in blood vials (vacutainers) and evacuated to $<1x10^{-3}$ Torr. Carbonate was hydrolised using 85% orthophosphoric acid, injected into the vacutainers, and the reaction was expedited by heating to 90°C. The resultant CO_2 was cryogenically purified and reduced to graphite at 570°C in the presence of iron catalyst and a stoichiometric excess of hydrogen following the methodology of Vogel et al., (1984; 1987).

$$CO_2 + 2H_2 \xrightarrow{570°C+Fe} C + 2H_2O$$

The graphite-iron mixtures were pressed into individual aluminum cathodes (target holders) and their ^{14}C content determined via accelerator mass spectrometry. Data were reported as fraction modern and conventional radiocarbon age (years BP) according to the convention put forth in Stuiver and Polach (1977), including a background correction based on ^{14}C-free calcite, and an average, estimated $\delta^{13}C$ value of 1.34±.0029‰.

Calibration to calibrated ages (putatively calendar years) were determined using Oxcal Version 4.2 (Ramsey, 2009; Reimer et al., 2013). Specifically, the original measurements were calibrated against the Marine 13 calibration curve, the most recent version of the internationally recognized radiocarbon calibration curve for pre-bomb ages (Reimer et al., 2013). Due to irregular mixing of oceanic waters, carbon isotope ratios vary spatially, requiring corrections for regional offset in radiogenic carbon from the global average used in the Marine 13 curve (e.g., Stuiver et al., 1986; Ulm, 2006).

James Busch created a code for Oxcal v4.2 (Ramsey, 2009; Reimer et al., 2013) that accounts for the post-bomb local/regional offset in radiogenic carbon at Coral Gardens using data from nearby Glovers Reef (16° 50' N, 87° 50' W) (Fig. 8) (Druffel 1981).

U-Th Sample preparation

Coral fragments (approximately 1 cm^3) were prepared for high-precision U-Th dating following rigorous cleaning procedures previously described by Clark et al. (2014a) designed to eliminate detrital contaminants with high concentrations of ^{232}Th within the aragonite skeleton. Each sample was crushed using a mortar and pestle and passed through a No. 18 1 mm grid sieve to separate grain size fractions. The 1 mm sized fragments were soaked overnight in a glass beaker containing a solution of 10% H_2O_2 (Fisher Scientific Certified ACS Hydrogen Peroxide) mixed in Milli-Q water (Millipore S.A.S. 67120 Molsheim). Between crushing each sample, the

mortar, pestle, No.18 sieve, and pan, were sonicated, rinsed with deionized water and dried with an air compressor (8 gal. 1.8 HP Kobalt) to minimise cross-contamination. After soaking the coral fragments overnight, samples were rinsed with Milli-Q water whilst still in the glass beakers and transferred to 50 mL Teflon centrifuge tubes. Fragments were re-submerged in 10% H_2O_2 solution and centrifuged for 15 min at 4000 rpm (Epindorf 5810R) in the Washington and Lee Biology Department. Residual hydrogen peroxide solution was carefully extracted with a pipette. Remaining fragments were rinsed with Milli-Q water and sonicated multiple times until the water solution was clear. Residual water was pipetted from the samples and fragments dried on a hotplate at 40^{o} C. Each sample was examined and photographed using a high-resolution binocular microscope (Olympus IX51 // Nixon DS-U2) and 500 mg of clean, unaltered aragonite fragments were selected for U-Th dating (Fig. 4; Fig. 5).

U-Th Chemistry

Samples were shipped to The University of Queensland where they underwent chemical preparation in clean conditions at the Radiogenic Isotope Facility following similar methods described by Clark et al (2014a, b). For each sample approximately 0.03 g of a ^{229}Th-^{233}U mixed tracer (^{226}Th-^{233}U-spike #2) was added to a pre-cleaned Teflon beaker using a pipette, the weight recorded, and then dried on a hot plate at 60 °C. Approximately 0.15 g of sample material was then added to the Teflon breaker with the dried products from the tracer. The combined tracer-sample mix was then dissolved in double-distilled 70% HNO_3 and 6-7 drops of H_2O_2 added to remove organics. Uranium and thorium were then separated and purified using ion-exchange column chemistry procedures modified from Edwards et al. (1987) and collected in a pre-cleaned 3.5 ml tube. As the Thorium separate solution contains a small fraction of U, all Th separate solutions were screened on a Quadrupole ICP-MS at the Radiogenic Isotope Facility, The

University of Queensland, to determine the concentration of U prior to measurement on the MC-ICP-MS. Screening solutions were prepared by diluting 50 µl of the Th stock solution in 4950 µl of 2% HNO_3. The solution was shaken to ensure complete homogenization and centrifuged for 20 min prior to measurement. Screening was performed to calculate the amount of U to be added to the Th separate in order to achieve 3-4 volts of ^{238}U signal on the MC-ICP-MS. Where U concentrations were low, a calculated volume of U from the U separate (based on average U concentrations in the U separate solutions) would be added to the Th separate. Solutions were then centrifuged at 4000 rpm for 20 minutes to draw out any resin that may have passed through the columns and collected in the 3 ml tube.

MC-ICP-MS Measurements

All 35 samples from Coral Gardens were dated using a Nu Plasma Multi-Collector Inductively Coupled Plasma Mass Spectrometer (MC-ICP-MS) at the Radiogenic Isotope Facility, The University of Queensland, specifically tailored for measuring young (<100 years old) coral samples. This instrument has a deceleration lens behind one of the two active secondary electron (SEM) multipliers to substantially increase abundance sensitivity. . The 2% HNO_3 solution containing both U and Th was drawn up by a Cetac ASX-110 auto-sampler and injected into the MC-ICP-MS using a DSN-100 desolvation nebulizer system. U-Th isotopes were measured in three sequences following Clark et al (2014a, b) over a time-span of about 25 minutes per sample.

Carry-over memory was minimized by flushing the auto-sampler for 15 minutes with 5% Aqua regia then 2% HNO_3 solution between samples. To account for machine drift, ^{229}Th and ^{233}U tracers were added into a separate dilute solution of a uranium oxide impurity standard New

Brunswick Laboratory 6 (NBL-6). This standard solution was measured every six samples to keep track of and later correct for machine drift.

Two-Component Correction Scheme

The presence of non-radiogenic (or initial) ^{230}Th) needs to be taken into consideration and corrected for in order to obtain reliable U-Th age estimates. In this study, U-Th age data was corrected for two isotopically distinct sources of non-radiogenic ^{230}Th ($^{230}Th_0$), soluble and insoluble, using a two-component mixing model described by Clark et al. (2014a). Insoluble $^{230}Th_0$ is incorporated into the skeletal matrix of the coral either during the growth or post-mortem, while soluble $^{230}Th_0$ can only be absorbed into the coral skeleton during growth. It is worth noting that both sources of non-radiogenic Th can be incorporated during development of the coral skeleton.. As site specific $^{230}Th_0$ values are yet to be determined for Coral Gardens, soluble and insoluble $^{230}Th_0$ values obtained from the Great Barrier Reef were used.

Results

Sample Information									
Location	Total Samples	Cross Dated	^{14}C Dated	XRD Verified	SEM Verified	U-Th Dated	XRD Verified	SEM Verified	Stable Isotopes
Dead Assemblage	191	2	39	35	10	10	4	6	24
Modern Canopy	41	24	23	4	3	24	5	5	25

Forty-one aragonite fragments were extracted from the modern canopy (Transect 5) and 191 from the dead assemblage (Pits A, B, and C). Thirty-nine pure samples from the dead assemblage were selected for radiocarbon dating (Fig. 8). Thirty-five of these samples were analyzed using the XRD and 10 with the SEM to verify aragonite quality of the sample population (Fig. 1). Twenty-three samples from the modern canopy were selected for radiocarbon dating. Four of these samples were analyzed with the XRD and three with the SEM.

The sample population from the modern canopy required less quality control analysis (XRD, SEM, and Microscope) than that of the dead assemblage sample due to less exposure to bio-erosion and encrustation.

		Radiocarbon Ages (Years)		
Location	Population Size (n)	Maximum of Median Age	Minimum of Median Age	Average Age Range (2σ)
Dead Assemblage	38	1973	1910	45.1
Modern Canopy	23	1973	1970	6.0

Age ranges with 2σ error were plotted on the regional radiocarbon calibration curve in Figure 8. Ten high-quality fragments from the dead assemblage were selected for high precision U-Th dating (Fig. 6). Five of these samples were analyzed in advance using the XRD and SEM. Each sample that was U-Th dated was also inspected beneath a binocular microscope and contaminants were removed to increase sample quality.

Twenty-five samples from the modern canopy were selected for U-Th dating (Fig. 6). Five samples underwent quality-check with the XRD, SEM, and binocular microscope. Ten samples were U-Th dated from the dead assemblage. Four were analyzed with the XRD and 6 with the SEM.

27 total samples were dated using both radiocarbon and U-Th methods. Twenty-two of which were from the modern canopy and 5 were from the dead assemblage. Eleven of these cross-dated samples from the modern canopy fell between the age range from 1977 to 1996.8 (Fig. 7). The oldest coral from the base of Pit C at the dead assemblage was 1915.3 ± 1.6 in age (Fig. 6).

		U-Th Ages (Years)		
Location	Population Size	Maximum	Minimum	Average Standard Error (2σ)
Dead Assemblage	10	1996.8	1915.3	1.6
Modern Canopy	24	2015.0	1982.7	1.1

Discussion and Conclusion

Sample Ages and Dating

The upper temporal limit of the regional radiocarbon calibration dataset is 1977 as seen in Figure 8 (Druffel, 1981; Ramsey, 2009 Oxcal v4.2; Reimer et al., 2013). This limit lead us to explore high-precision U-Th dating for aging modern aragonite samples younger than 1977 in age. Out of the 35 samples U-Th dated, one from the modern canopy was identified as an outlier. We were able to identify this outlier because it was also radiocarbon dated, and when plotted on the regional calibration curve, its age is clearly inconsistent with any possible values (red point in Figure 7). This outlier could be attributed to samples being mislabeled or inadequately cleaned aragonite material. Impurities could contribute high amounts of carbon-12 to the analysis, creating an apparent age much older than the true value.

Interpretations

Although not widely reported in peer-reviewed literature, many have endorsed the idea that modern populations of *A. cervicornis* must have repopulated current locations after the 1980s die-off. Results from this study suggests otherwise. Data show that *A. cervicornis* growth at Coral Gardens persisted through the well-known 1980s die-off (Fig. 6). This observation supports the idea that Coral Gardens is a legitimate ecological refugia for *A. cervicornis*. Keppel et al., (2012) defines an ecological refugia as a habitat with conditions that increase survival rates of a species that is under stress from changing environmental conditions. High-precision U-Th data (Clark et al., 2014a) and conventional radiocarbon data from this study can also be used to

extend the regional radiocarbon dataset that is corrected from the global marine average (Fig. 7) (Druffel, 1981; Ramsey, 2009 Oxcal v4.2; Reimer et al., 2013).

Ecological Refugia

Rather than capturing the state of *A. cervicornis* at Coral Gardens at a snap shot in time, we analyzed temporal coral presence with radiocarbon and high-precision U-Th dating. The oldest coral from the base of the dead assemblage was 1915.3 ± 1.6 and the youngest was 1996.8 ± 1.6 taken from the reef surface (Appendix B Table 1; Fig. 6). The oldest coral from within the modern canopy was 1982.7 ± 1.1 and the youngest was 2015 ± 0.9 (Appendix B Table 1; Fig. 6). This approximate 14 year overlap between the two sites supports the theory that *A. cervicornis* growth was continuous at Coral Gardens through the critical period of the late 1970s and early 1980s when most other populations of *A. cervicornis* declined. The oldest sample from the dead assemblage suggests that *A. cervicornis* survived at this location for nearly one decade after the onset of white band disease in this region (Fig. 6). Additionally, radiocarbon and U-Th data support that *A. cervicornis* growth was continuous at the current dead assemblage area up to the point of mortality in the late 1990s.

If *A. cervicornis* had been wiped-out at Coral Gardens during the early 1980s, then no existing corals would have been present in the area and new populations would have had to originate from sexual reproduction. The chances of this occurring are low because *A. cervicornis* relies primarily on asexual reproduction through fragmentation (Bruckner, 2003; NOAA, 2014). Fragmentation is a process where branches of *A. cervicornis* break off existing corals and grow nearby on habitable substrate (NOAA, 2014). If an area becomes barren of *A. cervicornis*, its chances of repopulating are low because there are no nearby corals to proliferate asexually (Bruckner, 2003). Information about poor sexual-reproduction coupled with high-precision U-Th

aging data give strength to the argument that *A. cervicornis* persisted through the 1980s die-off at Coral Gardens.

Radiocarbon Calibration Curve Extension

Prior to the application of high-precision carbonate dating with U-Th techniques, we were incapable of chronologically constraining significant events in the modern for *A. cervicornis* at Coral Gardens. Existing radiocarbon data for the region from Druffel (1981) was used to create a calibration curve that is applicable only to corals older in age than 1977 (Fig. 8) (Ramsey, 2009 Oxcal v4.2; Reimer et al., 2013*)*. By aging 26 samples with both radiocarbon and U-Th analyses, 24 of which were from the modern canopy, we can compare carbon fractionation ratios to actual U-Th ages to extend the regional dataset past 1977. Figure 6 displays how 14 samples that were cross-dated fill the time gap from 1977-2015 with medium-resolution when plotted on the existing regionally corrected calibration curve (Druffel, 1981). The horizontal positions of the data points were based on U-Th ages of cross-dated samples, plotting in the range from 1977-2015. The vertical position of cross dated ages reflect carbon isotope fractionation ratios obtained from radiocarbon dating. When all 14 cross-dated samples are plotted on the same graph as the regionally corrected calibration curve (Ramsey, 2009 Oxcal v4.2; Reimer et al., 2013) produced from Druffel's (1981) dataset, a noticeable trend of declining carbon isotope fractionation ratios after approximately 1977 becomes evident (Fig. 6).

Comparable trends can be seen in other carbon isotope ratio datasets. For example, Figure 16 displays radiocarbon isotope ratio data from different studies compiled by Bruun et al. (2005). Although these data from Bruun et al. (2005) reflect trends in carbon isotope ratios of terrestrial organics in equilibrium with radiogenic carbon in atmospheric reservoirs, similar trends in carbon isotope ratios are visible in the extended, regionally corrected curve (Druffel,

1981; Ramsey, 2009 Oxcal v4.2; Reimer et al., 2013). There is a temporal offset in key events, such as the peak in carbon isotope ratios, between the two graphs constructed from marine and atmospheric datasets. Fluctuations in atmospheric carbon isotope ratios take approximately one decade to equilibrate in marine reservoirs (Guilderson, personal communication). Despite the decadal delay, general trends in carbon isotope ratios are very similar between our the extended, regionally corrected curve (Druffel, 1981; Ramsey, 2009 Oxcal v4.2; Reimer et al., 2013) and the terrestrial dataset compiled by Bruun et al., (2005). This similarity helps verify the accuracy in ages and carbon isotope ratios of our cross-dated samples that were used to extend the regionally corrected radiocarbon dataset (Druffel, 1981; Ramsey, 2009; Reimer et al., 2013)

Summary

This study is the first to suggest that Coral Gardens is a legitimate ecological refugia. This claim is significant because Coral Gardens can be used as a location to conduct future studies directed towards promoting the recovery of *A. cervicornis* in the Caribbean. For example, one could characterize the hydrological conditions of Coral Gardens as an attempt to determine what specific details about the environment promote survival of *A. cervicornis*. Results from such a study could potentially be applied to construct artificial reefs or transplant *A. cervicornis* into environments with similar conditions. Modern populations of *A. cervicornis* at Coral Gardens could also be analyzed to determine if this specific strain is genetically unique and if its survival can be attributed to natural selection. For many reasons, Coral Gardens should be strongly considered to be a Marine Protected Area. Studies such as those mentioned above would likely take years to complete. Additionally, as one of the last remaining sites in the Caribbean to study an abundance of *A. cervicornis*, precautionary actions should be taken to protect this

ecological refugia from destructive impacts caused by anthropogenic disturbances (Busch, *Thesis*).

The extended regional calibration curve (Druffel, 1981; Ramsey, 2009 Oxcal v4.2; Reimer et al., 2013) for radiocarbon analysis has significant practical application, as well. With a thorough, regionally corrected radiocarbon dataset, ecologists can accurately date ages of fish by analyzing internal otolith accretions for carbon isotope data (e.g.: Kalish, 1993). Additionally, radiocarbon analysis can be used to accurately date modern carbonates in this region now that a regional dataset corrected from the global marine average dataset is available.

Acknowledgements

This project was funded by the following funds and organizations at Washington and Lee University: Johnson Opportunity Grant, Summer Research Scholar Program, R. Preston Hawkins IV Award in Geology, and Department of Geology. Many thanks to Dr. Tom Guilderson for hosting me at Lawrence Livermore National Lab and for teaching me how to age carbonates with conventional radiocarbon dating. Additionally, we are tremendously thankful for Dr. Tara Clark providing the U-Th dates that were crucial to the success of our study. This project would not have been possible without help from Emily Falls for teaching me how to use the mass spectrometer, SEM, and XRD machines. Also, thank you to Hayden Yates for her help with information on mass spectrometry. Thank you very much to Jenn Biegel and Harry Lustig for their help in Belize and in the lab at Washington and Lee. Finally, I am very thankful for Dr. Lisa Greer's guidance and for introducing me to coral reefs. Most importantly, she taught me the importance of being passionate about my work through example.

Appendix A: Radiocarbon Tables

Table 1 Calibrated carbon isotope ratios and corresponding ages of samples from Transect 5 and from Pits A, B, C following calibration using Oxcal v4.2 (Ramsey, 2009; Reimer et al., 2013; Druffel 1981). Dr. Tom Guilderson completed the radiocarbon dating for these samples and James Busch assembled an Oxcal code (Ramsey 2009) with the Glovers Reef dataset (Druffel, 1981) that is regionally corrected from the global marine average (Reimer et al., 2013).

Sample Number	Sample Name	Location	Lower Age (AD)	Upper Age (AD)	Median Age (AD)	Acomb
1	F10a-BZ-CG-TW15	Modern Canopy	1966	1972	1970	85.6
2	F1a-BZ-CG-TW15	Modern Canopy	1966	1972	1970	85.6
3	F1b-BZ-CG-TW15	Modern Canopy	1966	1972	1970	85.6
4	F3a-BZ-CG-TW15	Modern Canopy	1966	1972	1970	85.6
5	F6a-BZ-CG-TW15	Modern Canopy	1966	1972	1970	89.2
6	F7a-BZ-CG-TW15	Modern Canopy	1966	1972	1970	85.6
7	F8a-BZ-CG-TW15	Modern Canopy	1966	1972	1970	85.6
8	F9a-BZ-CG-TW15	Modern Canopy	1966	1972	1970	85.6
9	T5Eb-BZ-CG-TW15	Modern Canopy	1966	1972	1970	85.6
10	T5Ed-BZ-CG-TW15	Modern Canopy	1966	1972	1970	85.6
11	T5Ee-BZ-CG-TW15	Modern Canopy	1966	1972	1970	85.6
12	T5Ef-BZ-CG-TW15	Modern Canopy	1966	1972	1970	85.6
13	T5Na-BZ-CG-TW15	Modern Canopy	1966	1972	1970	85.6
14	T5Nc-BZ-CG-TW15	Modern Canopy	1966	1972	1970	85.6
15	T5Sd-BZ-CG-TW15	Modern Canopy	1966	1972	1970	85.6
16	T5Sf-BZ-CG-TW15	Modern Canopy	1966	1972	1970	85.6
17	T5Si-BZ-CG-TW15	Modern Canopy	1966	1972	1970	85.6
18	T5Wa-BZ-CG-TW15	Modern Canopy	1966	1972	1970	85.6
19	T5Wb-BZ-CG-TW15	Modern Canopy	1966	1972	1970	85.6
20	T5Wc-BZ-CG-TW15	Modern Canopy	1966	1972	1970	85.6
21	T5We-BZ-CG-TW15	Modern Canopy	1966	1972	1970	85.6
22	35-BZ-CG-JB14	Modern Canopy	1966	1972	1970	85.6
23	43-BZ-CG-JB14	Modern Canopy	1968	1975	1973	79.6
24	2A-BZ-CG-JB14	Pit A	1966	1972	1970	85.6
25	35A-BZ-CG-JB14	Pit A	1968	1975	1973	79.8
26	36A-BZ-CG-JB14	Pit A	1968	1975	1973	79.6
27	39A-BZ-CG-JB14	Pit A	1966	1975	1970	79.3
28	40A-BZ-CG-JB14	Pit A	1966	1974	1970	74.8
29	41A-BZ-CG-JB14	Pit A	1968	1975	1973	79.6
30	2B-BZ-CG-JB14	Pit B	1966	1974	1970	74.6
31	3B-BZ-CG-JB14	Pit B	1966	1974	1970	77.3
32	6B-BZ-CG-JB14	Pit B	1966	1974	1970	74.6
33	8B-BZ-CG-JB14	Pit B	1966	1974	1970	74.6
34	14B-BZ-CG-JB14	Pit B	1966	1972	1970	85.6
35	17B-BZ-CG-JB14	Pit B	1966	1972	1970	85.6
36	18B-BZ-CG-JB14	Pit B	1966	1972	1970	85.6
37	22B-BZ-CG-JB14	Pit B	1961	1975	1966	78.4

38	25B-BZ-CG-JB14	Pit B	1960	1975	1966	76.4
39	29B-BZ-CG-JB14	Pit B	1961	1975	1966	78.0
40	30B-BZ-CG-JB14	Pit B	1904	1975	1947	81.9
41	34B-BZ-CG-JB14	Pit B	1903	1975	1947	82.7
42	35B-BZ-CG-JB14	Pit B	1936	1975	1964	76.1
43	37B-BZ-CG-JB14	Pit B	1938	1975	1965	75.8
44	39B-BZ-CG-JB14	Pit B	1961	1975	1966	78.0
45	39BQA-BZ-CG-JB14	Pit B	1961	1975	1966	78.1
46	40B-BZ-CG-JB14	Pit B	1875	1968	1933	97.4
47	A2a-BZ -CG-TW15	Pit C	1966	1972	1970	85.6
48	A1b-BZ-CG-TW15	Pit C	1966	1972	1970	85.6
49	I3a-BZ-CG-TW15	Pit C	1875	1967	1932	97.4
50	I9a-BZ-CG-TW15	Pit C	1875	1966	1927	97.3
51	K7a-BZ-CG-TW15	Pit C	1876	1968	1935	97.2
52	L5c-BZ-CG-TW15	Pit C	1892	1970	1945	88.1
53	L6a-BZ-CG-TW15	Pit C	1877	1969	1941	94.7
54	M4a BZ -CG-TW15	Pit C	1872	1964	1916	97.9
55	M4a-BZ-CG-TW15 9 (rep)	Pit C	1877	1968	1939	96.2
56	M6d-BZ-CG-TW15	Pit C	1875	1966	1927	97.3
57	M8a-BZ-CG-TW15	Pit C	1877	1970	1943	92.2
58	M8e BZ -CG-TW15	Pit C	1872	1964	1910	98.8
59	M8e-BZ-CG-TW15 (rep)	Pit C	1876	1968	1937	96.7
60	M8f-BZ-CG-TW15	Pit C	1876	1968	1934	97.3
61	M8f-BZ-CG-TW15 (rep)	Pit C	1875	1966	1928	97.3
62	M9a-BZ-CG-TW15	Pit C	1872.0	1964.0	1916	97.9

Table 2 Uncalibrated carbon isotope fractionation values for samples from the modern canopy (Transect 5) and dead assemblage (Pits A, B, and C). Standard error is standard deviation (2σ). These data were reported by Dr. Tom Guilderson at the Center for Accelerated Mass Spectrometry at Lawrence Livermore National Laboratory.

Sample Number	Sample Name	Sample Location	$\delta^{13}C$	Fraction Modern	±	$D^{14}C$	±	^{14}C age	±
1	F10a-BZ-CG-TW15	Modern Canopy	-2.2900	1.0556	0.0032	55.600	3.20	>Modern	
2	F1a-BZ-CG-TW15	Modern Canopy	-2.3400	1.0892	0.0028	89.200	2.80	>Modern	
3	F1b-BZ-CG-TW15	Modern Canopy	-2.3100	1.0891	0.0027	89.100	2.70	>Modern	
4	F3a-BZ-CG-TW15	Modern Canopy	-2.7200	1.0663	0.0028	66.300	2.80	>Modern	
5	F6a-BZ-CG-TW15	Modern Canopy	-0.9300	1.0052	0.0026	5.200	2.60	>Modern	25
6	F7a-BZ-CG-TW15	Modern Canopy	-0.6500	1.0536	0.0035	53.600	3.50	>Modern	
7	F8a-BZ-CG-TW15	Modern Canopy	-2.7000	1.0576	0.0026	57.600	2.60	>Modern	
8	F9a-BZ-CG-TW15	Modern Canopy	-2.2600	1.0751	0.0029	75.100	2.90	>Modern	30
9	T5Eb-BZ-CG-TW15	Modern Canopy	-2.1800	1.0719	0.0037	71.900	3.70	>Modern	25
10	T5Ed-BZ-CG-TW15	Modern Canopy	-2.0000	1.0589	0.0028	58.900	2.80	>Modern	

11	T5Ee-BZ-CG-TW15	Modern Canopy	-2.6700	1.0594	0.0026	59.400	2.60	>Modern	25
12	T5Ef-BZ-CG-TW15	Modern Canopy	-2.7600	1.0663	0.0026	66.300	2.60	>Modern	
13	T5Na-BZ-CG-TW15	Modern Canopy	-2.5900	1.0803	0.0026	80.300	2.60	>Modern	
14	T5Nc-BZ-CG-TW15	Modern Canopy	-2.8500	1.0887	0.0029	88.700	2.90	>Modern	
15	T5Sd-BZ-CG-TW15	Modern Canopy	-2.0000	1.1248	0.0030	124.800	3.00	>Modern	
16	T5Sf-BZ-CG-TW15	Modern Canopy	-1.3200	1.0937	0.0028	93.700	2.80	>Modern	
17	T5Si-BZ-CG-TW15	Modern Canopy	-1.0420	1.1112	0.0027	111.200	2.70	>Modern	25
18	T5Wa-BZ-CG-TW15	Modern Canopy	-2.2000	1.0605	0.0026	60.500	2.60	>Modern	
19	T5Wb-BZ-CG-TW15	Modern Canopy	-1.7800	1.0950	0.0027	95.000	2.70	>Modern	
20	T5Wc-BZ-CG-TW15	Modern Canopy	-2.0000	1.0909	0.0041	90.900	4.10	>Modern	
21	T5We-BZ-CG-TW15	Modern Canopy	-1.8400	1.0943	0.0027	94.300	2.70	>Modern	
22	35-BZ-CG-JB14	Modern Canopy	-3.0	1.0674	0.0037	67.400	3.70	>Modern	
23	43-BZ-CG-JB14	Modern Canopy	-3.0	1.1527	0.0040	152.700	4.00	>Modern	
24	2A-BZ-CG-JB14	Pit A	-3.0	1.1234	0.0039	123.397	3.89	>Modern	
25	35A-BZ-CG-JB14	Pit A	-3.0	1.1571	0.0047	157.100	4.70	>Modern	
26	36A-BZ-CG-JB14	Pit A	-3.0	1.1559	0.0041	155.900	4.10	>Modern	
27	39A-BZ-CG-JB14	Pit A	-3.0	1.1427	0.0046	142.700	4.60	>Modern	
28	40A-BZ-CG-JB14	Pit A	-3.0	1.1388	0.0043	138.800	4.30	>Modern	
29	41A-BZ-CG-JB14	Pit A	-3.0	1.1578	0.0040	157.805	4.01	>Modern	
30	2B-BZ-CG-JB14	Pit B	-3.0	1.1288	0.0042	128.794	4.22	>Modern	
31	3B-BZ-CG-JB14	Pit B	-3.0	1.1430	0.0040	143.000	4.00	>Modern	
32	6B-BZ-CG-JB14	Pit B	-3.0	1.1358	0.0040	135.800	4.00	>Modern	
33	8B-BZ-CG-JB14	Pit B	-3.0	1.1319	0.0040	131.900	4.00	>Modern	
34	14B-BZ-CG-JB14	Pit B	-3.0	1.1026	0.0041	102.600	4.10	>Modern	
35	17B-BZ-CG-JB14	Pit B	-3.0	1.0944	0.0039	94.400	3.90	>Modern	
36	18B-BZ-CG-JB14	Pit B	-3.0	1.1026	0.0050	102.600	5.00	>Modern	
37	22B-BZ-CG-JB14	Pit B	-3.0	0.9773	0.0035	-22.700	3.50	185	30
38	25B-BZ-CG-JB14	Pit B	-3.0	0.9673	0.0034	-32.700	3.40	265	30
39	29B-BZ-CG-JB14	Pit B	-3.0	0.9718	0.0035	-28.200	3.50	230	30
40	30B-BZ-CG-JB14	Pit B	-3.0	0.9600	0.0034	-40.000	3.40	330	30
41	34B-BZ-CG-JB14	Pit B	-3.0	0.9608	0.0040	-39.200	4.00	320	35
42	35B-BZ-CG-JB14	Pit B	-3.0	0.9638	0.0034	-36.200	3.40	295	30
43	37B-BZ-CG-JB14	Pit B	-3.0	0.9646	0.0034	-35.400	3.40	290	30
44	39B-BZ-CG-JB14	Pit B	-3.0	0.9964	0.0036	-3.600	3.60	30	30
45	39BQA-BZ-CG-JB14	Pit B	-3.0	0.9977	0.0040	-2.300	4.00	20	35
46	40B-BZ-CG-JB14	Pit B	-3.0	0.9515	0.0033	-48.508	3.30	400	30
47	A2a-BZ -CG-TW15	Pit C	-2.0000	1.0862	0.0032	86.218	3.23	>Modern	
48	A1b-BZ-CG-TW15	Pit C	-1.2000	1.0868	0.0027	86.800	2.70	>Modern	
49	I3a-BZ-CG-TW15	Pit C	-1.6200	0.9509	0.0028	-49.100	2.80	405	25
50	I9a-BZ-CG-TW15	Pit C	-1.9100	0.9496	0.0028	-50.400	2.80	415	25
51	K7a-BZ-CG-TW15	Pit C	-0.2400	0.9515	0.0028	-48.500	2.80	400	25
52	L5c-BZ-CG-TW15	Pit C	-1.8000	0.9565	0.0028	-43.500	2.80	355	25
53	L6a-BZ-CG-TW15	Pit C	-0.7300	0.9536	0.0028	-46.400	2.80	380	25
54	M4a BZ -CG-TW15	Pit C	-1.6952	0.9462	0.0029	-53.839	2.94	445	25
55	M4a-BZ-CG-TW15 9 (rep)	Pit C	-1.7000	0.9527	0.0028	-47.300	2.80	390	25
56	M6d-BZ-CG-TW15	Pit C	-0.8900	0.9496	0.0028	-50.400	2.80	415	25
57	M8a-BZ-CG-TW15	Pit C	-1.4000	0.9555	0.0033	-44.500	3.30	365	30

58	M8e BZ -CG-TW15	Pit C	-1.3293	0.9436	0.0031	-56.414	3.05	465	30
59	M8e-BZ-CG-TW15 (rep)	Pit C	-1.3300	0.9523	0.0029	-47.700	2.90	390	25
60	M8f-BZ-CG-TW15	Pit C	-1.5600	0.9513	0.0028	-48.700	2.80	400	25
61	M8f-BZ-CG-TW15 (rep)	Pit C	-1.5600	0.9499	0.0028	-50.100	2.80	415	25
62	M9a-BZ-CG-TW15	Pit C	-1.6800	0.9460	0.0028	-54.000	2.80	445	25

Appendix B: U-Th Dating

Table 1 U-Th ages for samples from Transect 5 and Pit C. Standard error is standard deviation (2σ). * Denotes an outlier that was removed from the dataset. U-Th dating completed by Dr. Tara Clark.

Sample Number	Sample Name	Location	Year Corrected (AD)	Standard Error (±)
1	F10a-BZ-CG-TW15	Transect 5	2010.2	0.9
2	F10c-BZ-CG-TW15	Transect 5	2011.4	0.9
3	F1a-BZ-CG-TW15	Transect 5	1996.2	1.3
4	F1b-BZ-CG-TW15	Transect 5	1993.7	1.2
5	F3a-BZ-CG-TW15	Transect 5	2008.9	1.0
6	F6a-BZ-CG-TW15*	Transect 5	1931.6	2.6
7	F7a-BZ-CG-TW15	Transect 5	2015.0	0.9
8	F8a-BZ-CG-TW15	Transect 5	2009.2	0.9
9	F9a-BZ-CG-TW15	Transect 5	2005.0	1.0
10	T5Eb-BZ-CG-TW15	Transect 5	2005.7	1.1
11	T5Ed-BZ-CG-TW15	Transect 5	2008.5	1.0
12	T5Ee-BZ-CG-TW15	Transect 5	2008.4	1.0
13	T5Ef-BZ-CG-TW15	Transect 5	2008.3	1.1
14	T5Na-BZ-CG-TW15	Transect 5	2001.5	1.2
15	T5Nc-BZ-CG-TW15	Transect 5	2009.7	1.0
16	T5Sb-BZ-CG-TW15	Transect 5	1993.6	1.0
17	T5Sd-BZ-CG-TW15	Transect 5	1986.3	1.1
18	T5Sd-BZ-CG-TW15	Transect 5	1984.5	1.2
19	T5Sf-BZ-CG-TW15	Transect 5	1990.6	1.3
20	T5Si-BZ-CG-TW15	Transect 5	1982.7	1.3
21	T5Wa-BZ-CG-TW15	Transect 5	2003.3	1.1
22	T5Wb-BZ-CG-TW15	Transect 5	1992.3	1.1
23	T5Wc-BZ-CG-TW15	Transect 5	1994.3	1.1
24	T5Wd-BZ-CG-TW15	Transect 5	1988.7	1.2
25	T5We-BZ-CG-TW15	Transect 5	1994.5	1.1
26	A1b-BZ-CG-TW15	Pit C	1993.1	1.2
27	A2a-BZ-CG-TW15	Pit C	1996.8	1.2

28	A2b-BZ-CG-TW15	Pit C	1960.8	4.3
29	A6a-BZ-CG-TW15	Pit C	1986.4	1.1
30	D4a-BZ-CG-TW15	Pit C	1967.3	1.2
31	G3a-BZ-CG-TW15	Pit C	1950.2	1.3
32	J2a-BZ-CG-TW15	Pit C	1915.3	1.6
33	M4a-BZ-CG-TW15	Pit C	1916.4	1.4
34	M8a-BZ-CG-TW15	Pit C	1952.2	1.2
35	M8f-BZ-CG-TW15	Pit C	1921.3	1.5

Appendix C: Figures

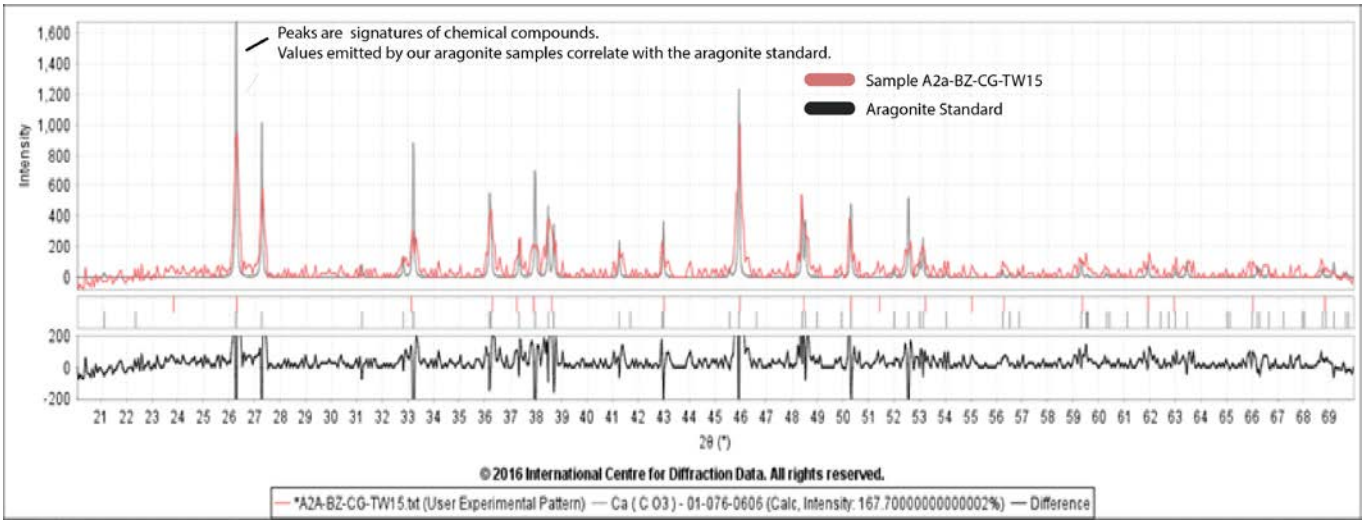

Figure 1 Example XRD analysis result. (Sample A2a-BZ-CG-TW15. Figured provided by Emily Falls.

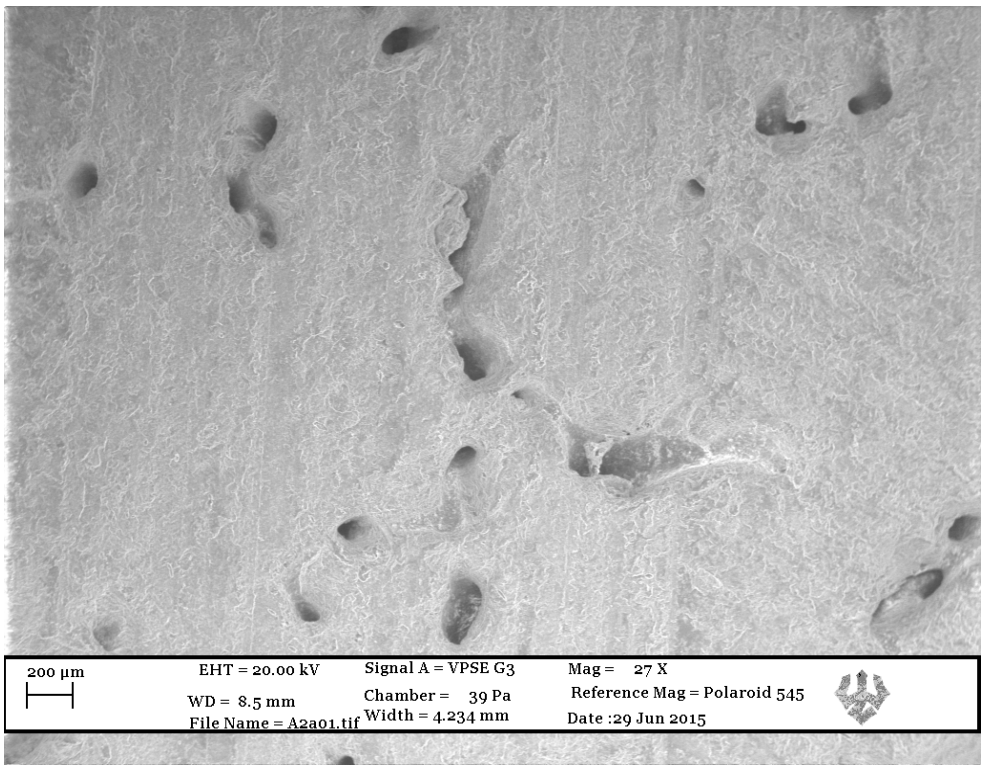

Figure 2 Clean aragonite slice beneath the SEM (Sample A2a-BZ-CG-TW15). Figure provided by Emily Falls.

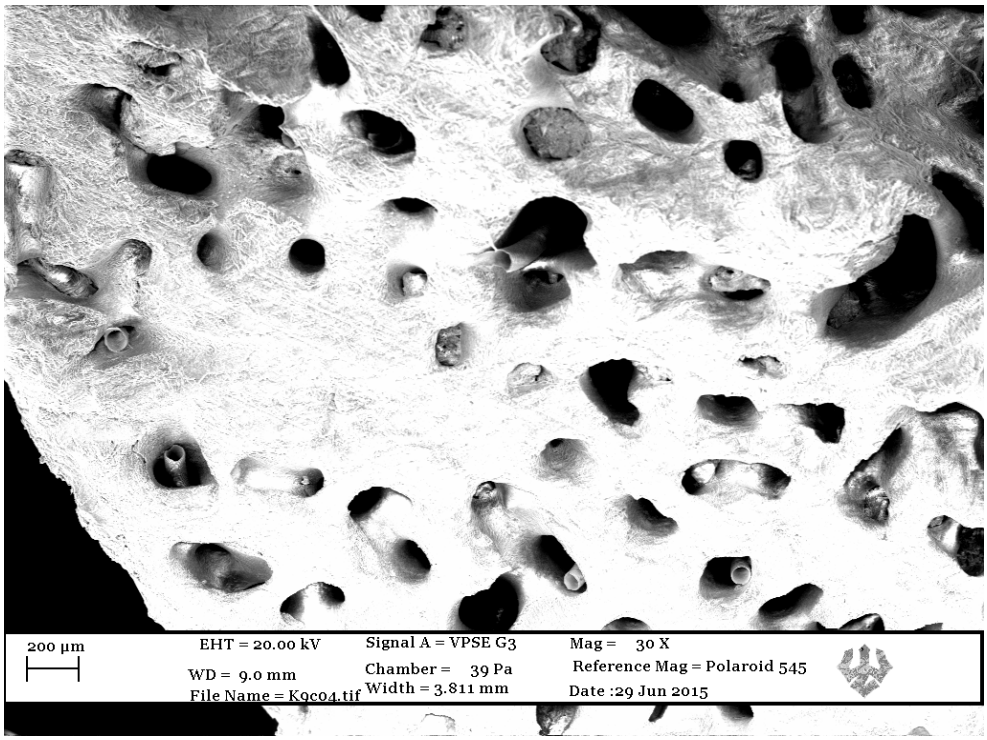

Figure 3 A low-quality aragonite sample being examined for organic impurities and calcite crystallization with the SEM (Sample K9c-BZ-CG-TW15). Figure provided by Emily Falls.

Figure 4 Clean aragonite fragments beneath the binocular microscope (Sample A2a-BZ-CG-TW15).

Figure 5 A contaminant settled between pure aragonite fragments being examined beneath the binocular microscope (Sample M8f-BZ-CG-TW15).

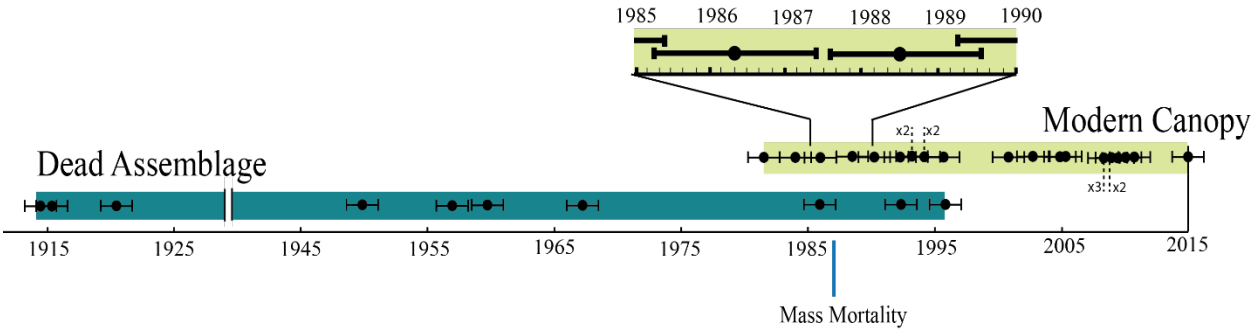

Figure 6 U-Th ages of samples from the dead assemblage (Pit C) and modern canopy. Notice the 14 year chronological overlap between the time that the dead assemblage was last living and the youngest age found representing the first growth of *A. cervicornis* at the modern canopy. U-Th dating completed by Dr. Tara Clark.

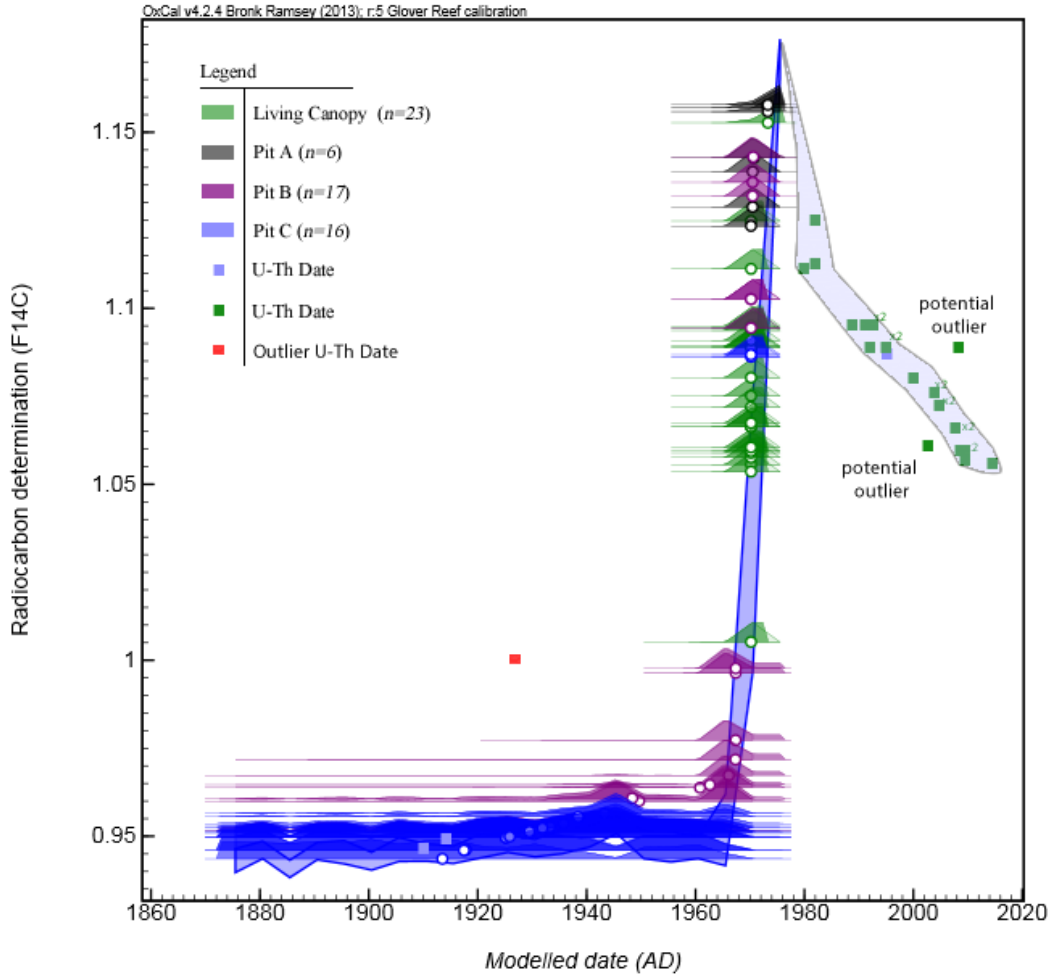

Figure 7 Data points of corals that were both radiocarbon and U-Th dated. If the data is high enough-resolution, we could possibly extend the radiocarbon calibration curve from 1977 to 2015 with future work. The red data point represents an outlier and was removed from the sample population (Sample F6a-BZ-CG-TW15) (Druffel 1981; Ramsey 2009 Oxcal v4.2; Reimer et al., 2013). Radiocarbon dating completed by Dr. Tom Guilderson. U-Th dating completed by Dr. Tara Clark.

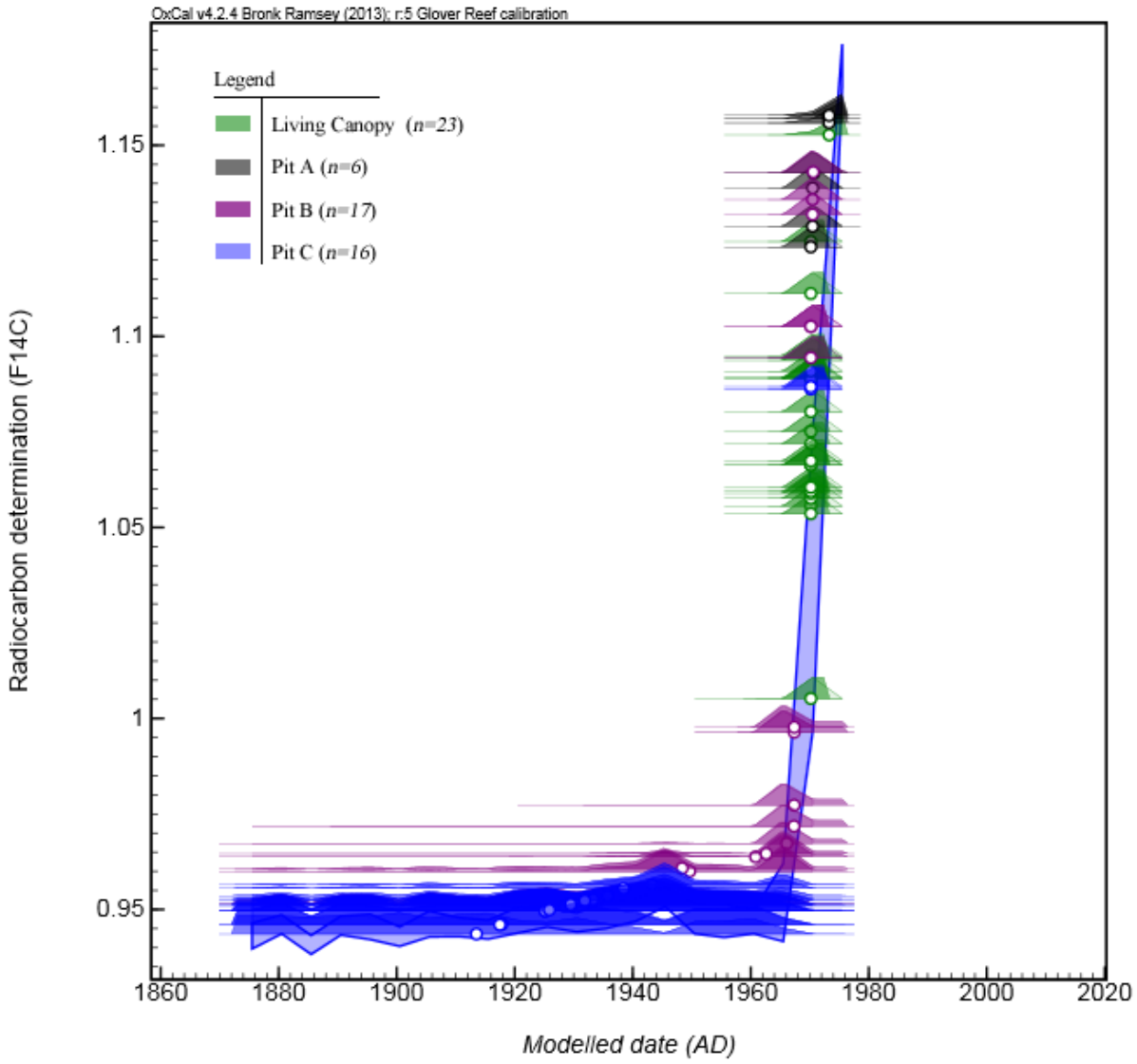

Figure 8 Radiocarbon dates of samples from the dead assemblage (Pits A, B, & C) and the modern, living canopy. The calibration curve is derived from radiocarbon data completed by Ellen Druffel (1981) from Glovers Reef, Belize. The maximum age of samples that can be dated with this curve is 1977 (Ramsey 2009 Oxcal v4.2; Reimer et al., 2013). Radiocarbon dating performed by Dr. Tom Guilderson.

Figure 9 An example *A. cervicornis* fragment encrusted with coralline algae. This picture was taken before the outer edges were removed using a tile saw (Sample A6-BZ-CG-TW15).

Figure 10 An example *A. cervicornis* fragment after the edges were trimmed-off using the tile saw.

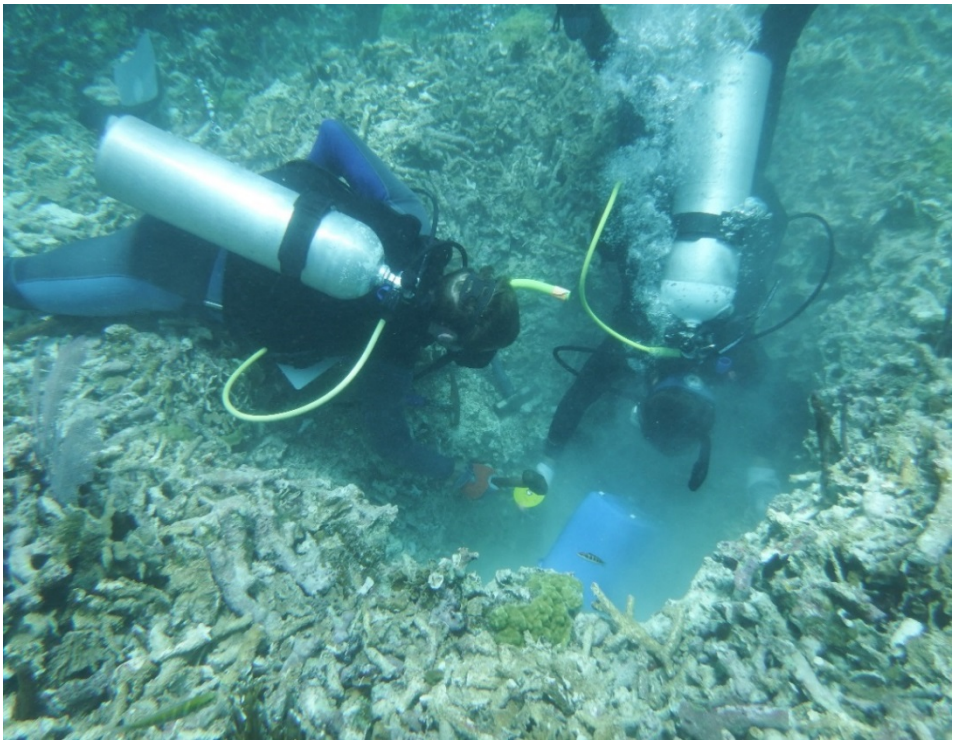

Figure 11 Two divers using a hammer and chisel to excavate Pit C in the dead assemblage. Photo taken by Jenn Biegel.

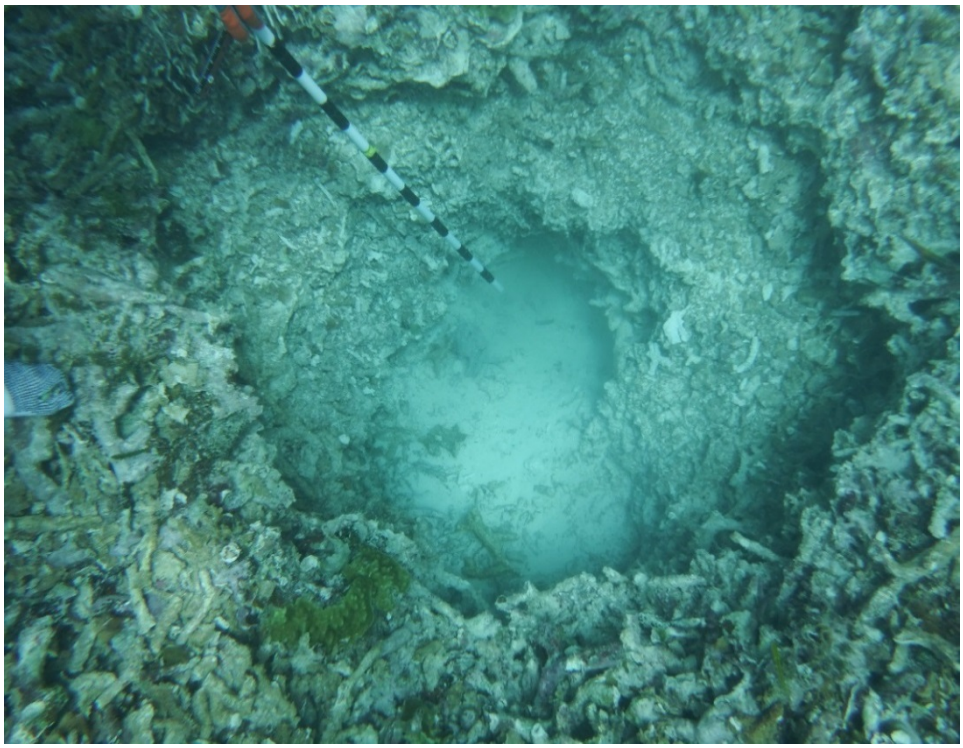

Figure 12 Overhead view of Pit C dug into the dead assemblage. Each segment on the stick is 10 cm in length. This picture was taken prior to the final excavation dive.

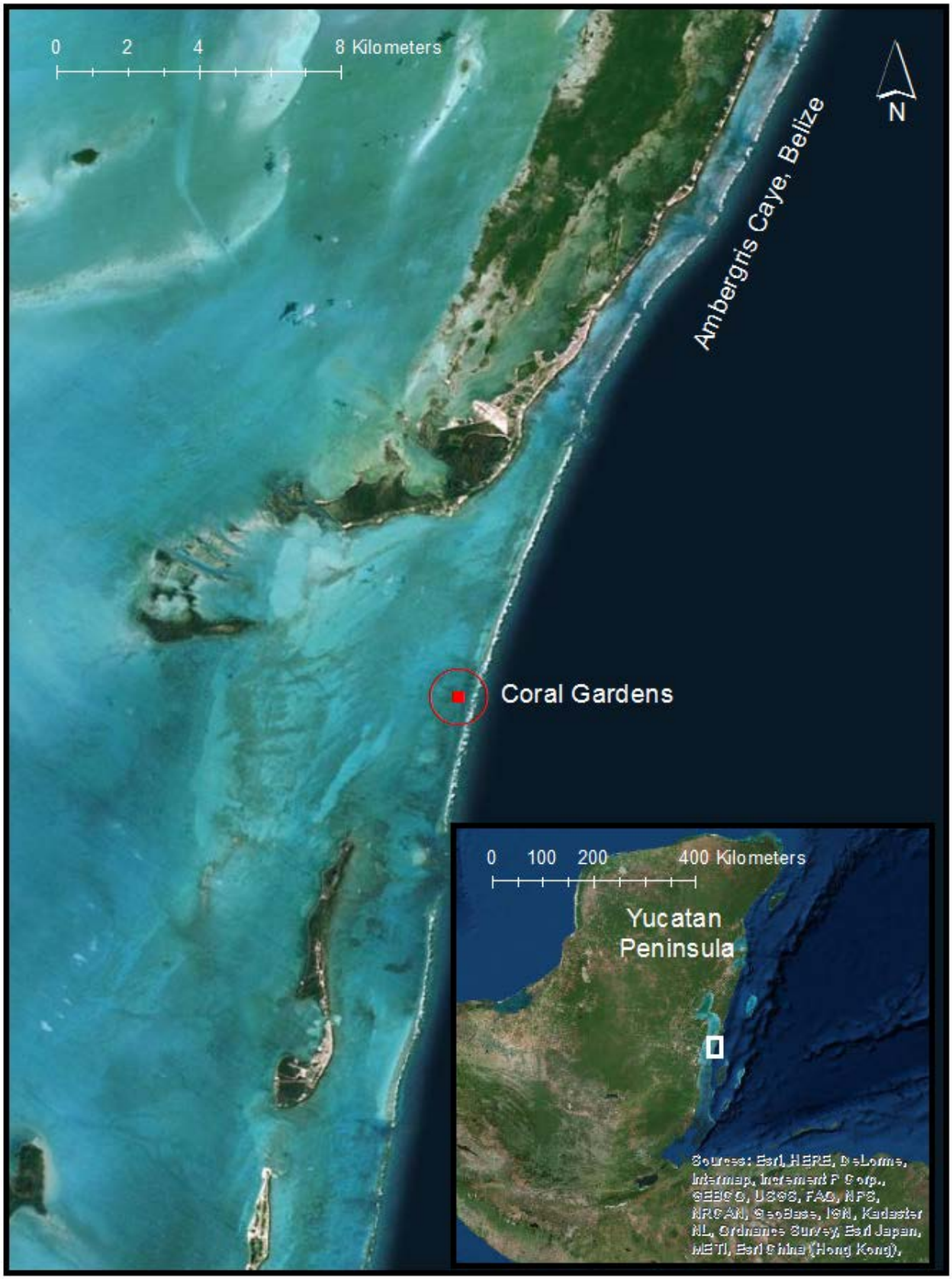

Figure 13 Study location. Coral Gardens [17° 49’ 54.7644”, 87° 59’ 29.9743”] is located in-shore of the Mesoamerican Barrier reef approximately 6 kilometers offshore the southern tip of Amergris Caye, Belize. Constructed using ArcGIS v10.3.2.

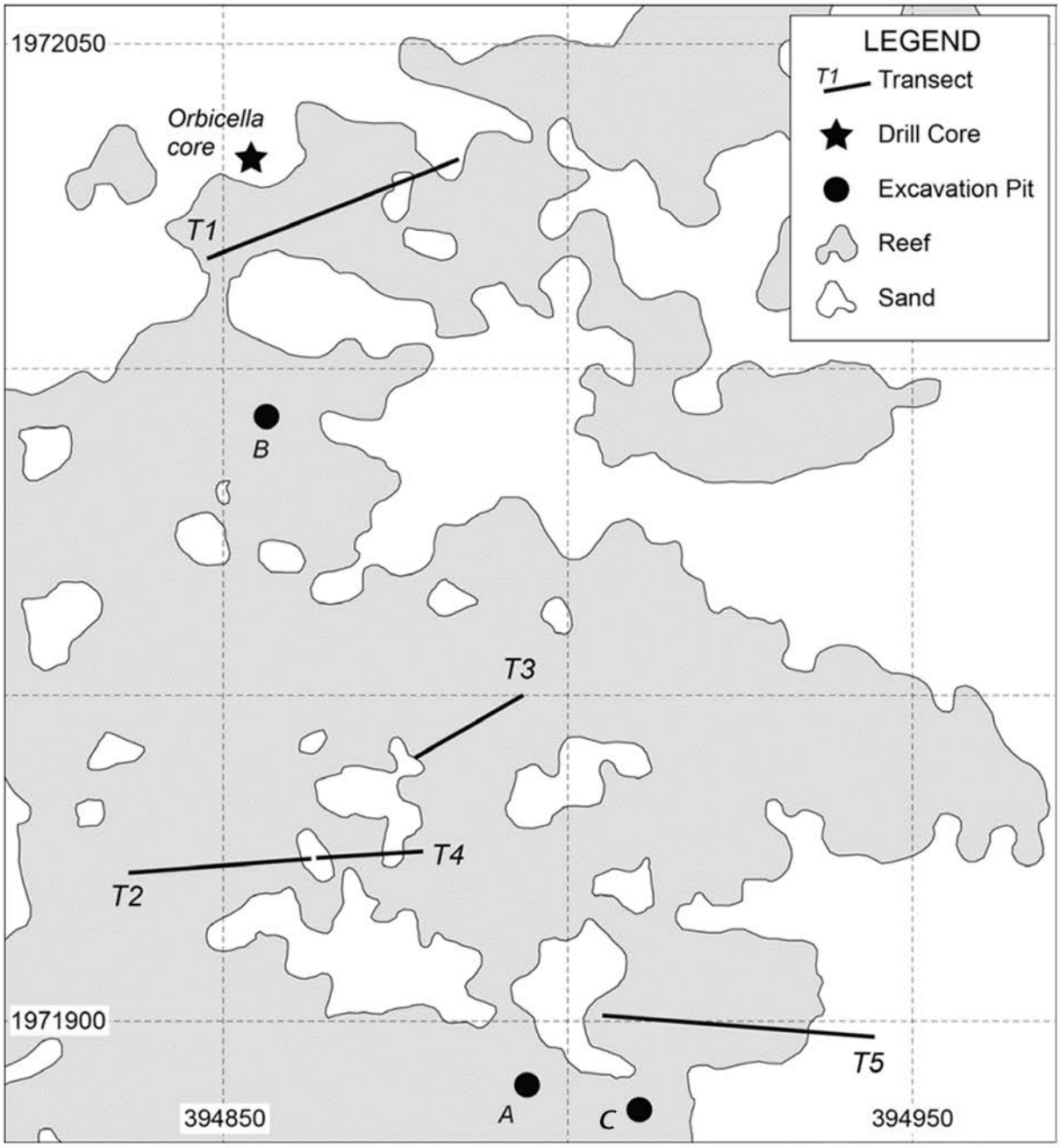

Figure 14 Map of Coral Gardens area. Pits A, B, and C were dug in sections of dead reef. All transects denote locations of modern populations of *A. cervicornis*. Modified from Greer et al., (2015).

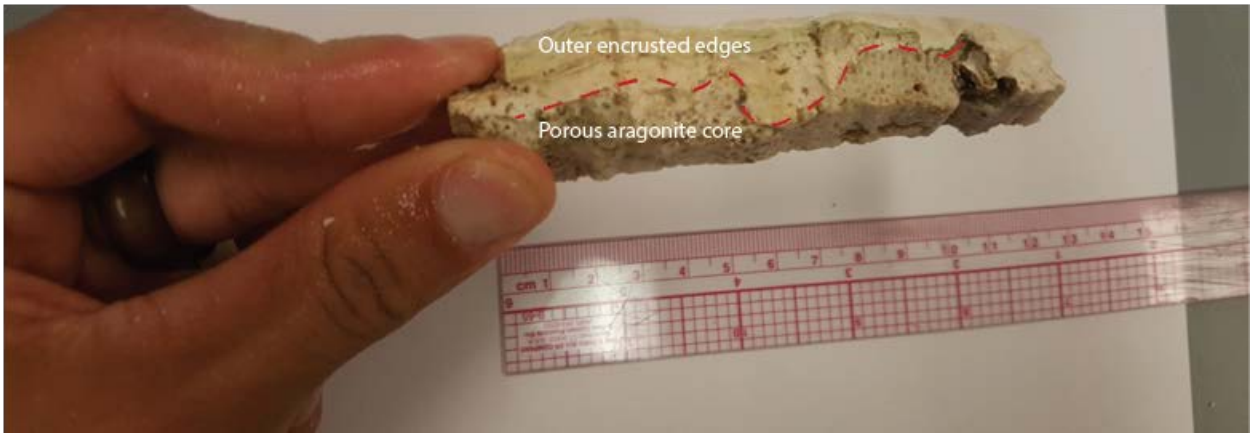

Figure 15 Photo taken by Harry Lustig. A coral fragment taken from the surface of Pit C in the dead assemblage. This coral has been cut cross sectionally to expose the outer encrusted layers and porous aragonite core. (Ssample A3a-BZ-CG-TW15)

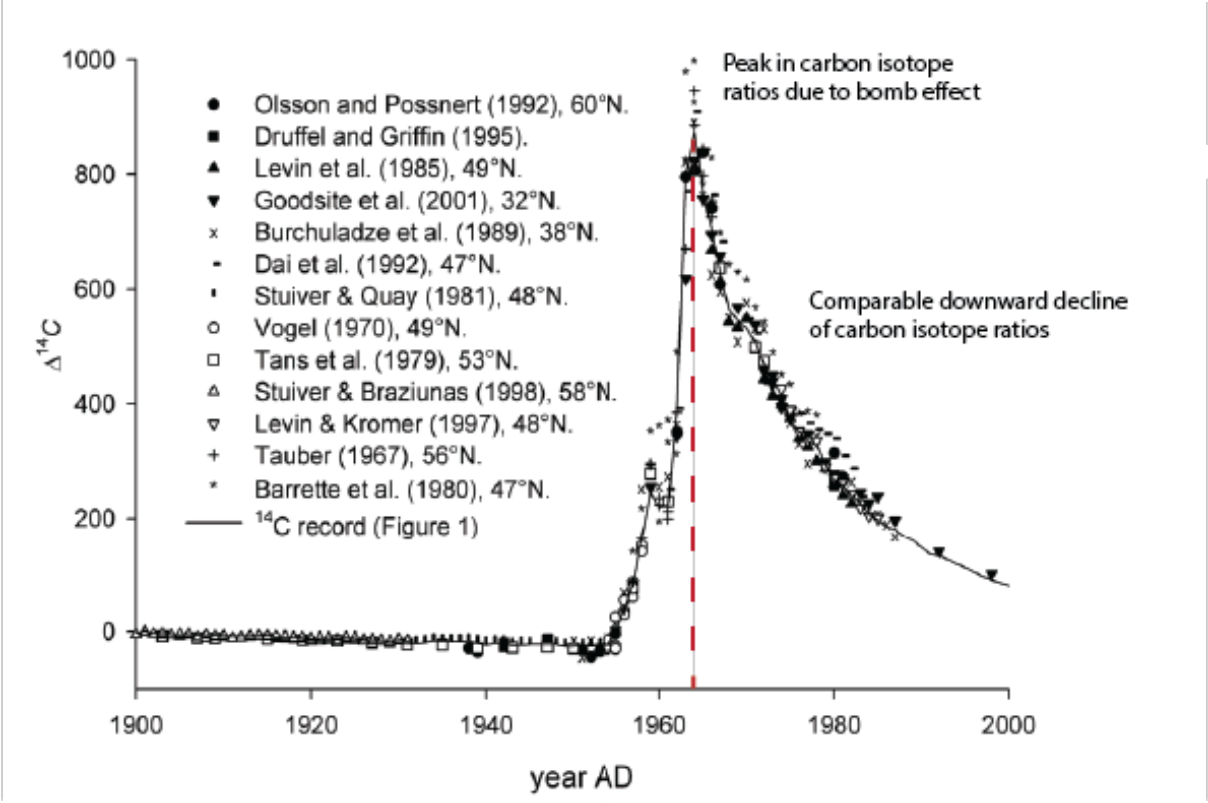

Figure 16 Modified from Bruun et al., (2005). Displays a comparable trend in carbon isotope ratios to that seen in Figure 7 for the extended regional radiocarbon calibration curve (Druffel, 1981; Ramsey 2009 Oxcal v4.2; Reimer et al., 2013).

Figure 17 Photo taken by James Busch. The modern canopy of *A. cervicornis* at Transect 5 (Fig. 14) in Coral Gardens, Belize

Figure 18 Photo taken by James Busch. An example of remnant *A. cervicornis* reefs at Coral Gardens. Excavation pits (A, B, and C) were dug at locations such as this.

References

Adey WH (1978) Coral reef morphogenesis: a multidimensional model. Science 202: 831–837

Aronson RB, Precht WF (2001) White-band disease and the changing face of caribbean coral reefs. Hydrobiologia, 460, 25-38. doi:10.1023/A:1013103928980

Aronson RB, Macintyre IG, Precht WF, Murdoch TJT, Wapnick CM (2002) The expanding scale of species turnover events on coral reefs in Belize: Ecological Monographs, v. 72, p. 233–249.

Aronson RB, Macintyre IG, Lewis SA, Hilbun NL (2005) Emergent zonation and geographic convergence of coral reefs. Ecology, 86(10), 2586-2600

Bruckner AW (2003) Proceedings of the Caribbean Acropora Workshop: potential application of the US Endangered Species Act as a conservation strategy. Silver Spring, Maryland: NOAA Technical Memorandum NMFS-OPR-24. 199 p.

Bruun S, Six J, Jensen LS, Paustian K (2005) Estimating turnover of soil organic carbon fractions based on radiocarbon measurements. Radiocarbon, 47(1), 99-113

Burke R, Walter A, MacIntyre I (1977) Overview of the Holocene History, Architecture, and Structural Components of Tague Reef and Lagoon. National Oceanic and Atmospheric Administration (NOAA). http://www.aoml.noaa.gov/general/lib/CREWS/Cleo/St.%20Croix/salt_river163.pdf

Busch J, Greer L, Harbor D, Wirth K, Lescinsky H, Curran HA, de Beurs K (in press) Quantifying exceptionally large populations of Acropora spp. corals off Belize using sub-meter satellite imagery classification. Bulletin of Marine Science. Vol 92, No 2. 2016

Busch J, Greer L (*thesis*) GeoEye-1 multispectral satellite imagery classification: An accurate method for identifying populations of *Acropora* spp. corals prior to a field study (2015 undergraduate geology thesis). Washington and Lee University, Lexington, VA

Clark TR, Roff G, Zhao J, Feng Y, Done TJ, Pandolfi JM (2014a) Testing the precision and accuracy of the U-Th chronometer for dating coral mortality events in the last 100 years. Quat. Geochronol. 23, 35-45.

Clark TR, Zhao J, Roff G, Feng Y, Done TJ, Nothdurft LD, Pandolfi JM (2014b) Discerning the timing and cause of historical mortality events in modern Porites from the Great Barrier Reef. Geochim. Cosmochim. Acta 138, 57-80

Cramer KL, Jackson JBC, Angioletti CV, Leonard-Pingel J, Guilderson TP (2012) Anthropogenic mortality on coral reefs in caribbean panama predates coral disease and bleaching. Ecology Letters, 15(6), 561-567. doi:10.1111/j.1461-0248.2012.01768.x

Davis GE (1982) A century of natural change in coral distribution at the Dry Tortugas: a comparison of reef maps from 1881 and 1976. Bulletin marine Science 32: 608–623.

Druffel EM (1981) Radiocarbon in annual coral rings from the eastern tropical pacific ocean. Geophysical Research Letters, 8(1), 59-62. doi: 10.1029/GL008i001p00059

Edwards RL, Chen JH, Wasserburg GJ (1987) 238U234U230Th232Th systematics and the precise measurement of time over the past 500,000 years. Earth and Planetary Science Letters, 81(2-3), 175-192. doi:10.1016/0012-821X(87)90154-3

Gardner TA, Côté IM, Gill JA, Grant A, Watkinson AR (2003) Long-term region-wide declines in caribbean corals. Science, 301(5635), 958-960. doi:10.1126/science.1086050

Gladfelter WB (1982) White-Band Disease in Acropora palmata-Implications for the structure and growth of shallow reefs. Bulletin of Marine Science 32: 639–643

Glynn PW (1993) Coral reef bleaching: Ecological perspectives. Coral Reefs, 12(1), 1-17. doi: 10.1007/BF00303779

Goreau TF, Goreau NI (1973) The ecology of Jamaican coral reefs. II. Geomorphology, zonation and sedimentary phases. Bull Mar Sci 23: 399–464.

Greenstein BJ, Curran HA, Pandolfi JM (1998) Shifting ecological baselines and the demise of *Acropora cervicornis* in the western north atlantic and caribbean province: A pleistocene perspective. Coral Reefs, 17(3), 249-261. doi : 10.1007/s003380050125

Greenstein BJ, Moffat HA (1996) Comparative taphonomy of modern and Pleistocene corals, San Salvador, Bahamas: PALAIOS, v. 11, p. 57–63, doi: 10.2307/3515116.

Greer L, Jackson JE, Curran HA, Guilderson TP, Teneva L, (2009) How vulnerable is *Acropora cervicornis* to environmental change? Lessons from the early to middle Holocene: Geology, v. 37, p. 263–266.

Greer L, Lescinsky H, Wirth K (2015) Multi-Level Characterization of Acroporid Coral Populations at Coral Gardens, Belize: A Refugia Identified. Keck Geology Consortium, 28th Annual Symposium: p. 6-11.

Guilderson TP (2016) Personal communication via phone. Washington and Lee University. Lexington, VA to Lawrence Livermore National Laboratory. Livermore, CA

Hubbard DK (1988) Controls of modern and fossil reef development: common ground for biological and geological research. Proc. 6th Int. Coral Reef Symp. 1: 243–252.

Huntington BE, Miller MW (2014) Location specific metrics for rapidly estimating the abundance and condition of he threatened coral *Acropora cervicornis*. Restor Ecol. 22:299–303. http://dx.doi.org/10.1111/rec.12057

Irwin A, Greer L, Humston R, Devlin-Durante M, Baums I, Lescinsky H, Wirth K, Cabe P, Curran HA (in review) Age and intraspecific diversity of resilient Acropora communities in Belize. Washington and Lee University. Lexington, VA.

Jackson JB, Kirby MX, Berger WH, Bjorndal KA, Botsford LW, Bourque BJ et al. (2001) Historical overfishing and the recent collapse of coastal ecosystems. Science, 292, 629–637.

Jackson, JBC (1992) Pleistocene Perspectives on Coral Reef Community Structure. American Zoologist, 32(6), 719–731.

Johnson KG, Budd A, Stenmann TA (1995) Extinction selectivity and ecology of Neogene Caribbean reef corals. Paleobiology 21: 52–73

Kalish JM (1993) Pre- and post-bomb radiocarbon in fish otoliths. Earth and Planetary Science Letters 114: 549–54

Keck J, Houston RS, Purkis S, Riegl BM (2005) Unexpectedly high cover of *Acropora cervicornis* on offshore reefs in Roatán (Honduras). Coral Reefs. 24:509. http://dx.doi.org/10.1007/ s00338-005-0502-6

Keppel G, Van Niel KP, Wardell-Johnson, GW, Yates CJ, Byrne M, Mucina L et al. (2012) Refugia: Identifying and understanding safe havens for biodiversity under climate change. Global Ecology and Biogeography, 21(4), 393-404. doi:10.1111/j.1466-8238.2011.00686.x

Kline DI, Vollmer SV (2011) White band disease (type I) of endangered caribbean acroporid corals is caused by pathogenic bacteria. Scientific Reports, 1 doi: 10.1038/srep00007

Knowlton N, Lang JC, Keller BD (1990) Case study of natural population collapse: post-hurricane predation on Jamaican staghorn corals. Smithsonian Contrib. mar. Sci. 31: 1–25.

Larson EA, Gilliam DS, Padierna ML, Walker BK (2014) Possible recovery of Acropora palmata (Scleractinia: Acroporidae) within the Veracruz Reef System, Gulf of Mexico: asurvey of 24 reefs to assess the benthic communities. Rev Biol Trop 62 (3): 75-84

Lessios HA (1988) Mass mortality of Diadema antillarum in the Caribbean: what have we learned? Ann. Rev. Ecol. Syst. 19: 371–393.

Lidz BH, Zawada DG (2013) Possible return of *Acropora cervicornis* at Pulaski Shoal, Dry Tortugas National Park, Florida. J Coast Res. 29:256–271. http://dx.doi.org/10.2112/JCOASTRES-D-12-00078.1

Lirman D, Bowden-Kerby A, Schopmeyer S, Huntington B, Thyberg T, Gough M, Gough Y (2010) A window to the past: documenting the status of one of the last remaining ‘megapop-ulations’ of the threatened staghorn coral *Acropora cervicornis* in the Dominican Republic. Aquat Conserv: Mar and Freshwat Ecosystems. 20:773–781.

Macintyre IG, Burke RB, Stuckenrath R (1977) Thickest recorded holocene reef section, isla pérez core hole, alacran reef, mexico. Geology, 5(12), 749-754. doi: 10.1130/0091-7613(1977)5<749:TRHRSI>2.0.CO;2

Manz LA (2015) Carbon-14. Department of Mineral Resources (DMR). https://www.dmr.nd.gov/ndgs/documents/newsletter/Winter%202015/Carbon-14.pdf

Mesollela KJ (1967) Zonation of uplifted Pleistocene coral reefs on Barbados, West Indies. Science 156: 638–640

Miller MW, Bourque AS, Bohnsack JA (2002) An analysis of the loss of acroporid corals at looe key, florida, USA: 1983-2000. Coral Reefs, 21(2), 179-182

Newell ND, Rigby JK (1957) Geological studies on the Great Bahama Bank. In: R.J. Le Blanc and J.G. Breeding (Editors), Regional Aspects of Carbonate Deposition. Soc. Econ. Paleontol. Mineral. Spec. Publ., 5: 15-72

National Oceanic and Atmospheric Administration, NOAA (2014) Staghorn Coral (*Acropora cervicornis*). http://www.nmfs.noaa.gov/pr/species/invertebrates/staghorncoral.htm

National Oceanic and Atmospheric Administration, NOAA (2015) Staghorn Coral (*Acropora cervicornis*). http://www.fisheries.noaa.gov/pr/species/invertebrates/coral/staghorn-coral.html

Pandolfi JM, Jackson JBC (2006) Ecological persistence interrupted in caribbean coral reefs. Ecology Letters, 9(7), 818-826. doi:10.1111/j.1461-0248.2006.00933.x

Pandolfi JM, Bradbury RH, Sala E, Hughes TP, Bjorndal KA, Cooke RG et al. (2003) Global trajectories of the long-term decline of coral reef ecosystems. Science, 301, 955–958.

Porter JW, Battey JF, Smith JG (1982) Perturbation and change in coral reef communities. Proc natn. Acad. Sci. U.S.A.79: 1678–1681.

Purkis SJ, Myint SW, Riegl BM (2006) Enhanced detection of the coral *Acropora cervicornis* from satellite imagery using a textural operator. Remote Sens Environ. 101:82–94. http:// dx.doi.org/10.1016/j.rse.2005.11.009

Ramsey CB (2009) Bayesian analysis of radiocarbon dates. Radiocarbon, 51(1), 337-360. Used in application: Oxcal Version 4.2.

Randall CJ, Van Woesik R (2015) Contemporary white-band disease in caribbean corals driven by climate change. Nature Climate Change, 5(4), 375-379. doi: 10.1038/nclimate2530

Reimer PJ, Bard E, Bayliss A, Beck JW, Blackwell PG, Bronk-Ramsey C, Grootes PM, Guilderson TP, Haflidason H, Hajdas I, HattŽ C, Heaton TJ, Hoffmann DL, Hogg AG, Hughen KA, Kaiser KF, Kromer B, Manning SW, Niu M, Reimer RW, Richards DA, Scott EM, Southon JR, Staff RA,

Turney CSM, van der Plicht J (2013) IntCal13 and Marine13 Radiocarbon Age Calibration Curves 0-50,000 Years cal BP. Radiocarbon, 55(4).

Rogers CS (1993) Hurricanes and coral reefs: The intermediate disturbance hypothesis revisited. Coral Reefs, 12(3-4), 127-137. doi:10.1007/BF00334471

Rosenzweig C, Karoly D, Vicarelli M, Neofotis P, Wu Q, Casassa G, Menzel A, Root TL, Estrella N, Seguin B, Tryjanowski P, Liu C, Rawlins S, Imeson A (2008) Attributing physical and biological impacts to anthropogenic climate change. Nature, vol. 453, pp. 353–57

Shinn EA, Reich CD, Hickey TD, Lidz BH (2003) Staghorn tempestites in the Florida Keys: Coral Reefs, v. 22, p. 91–97, doi: 10.1007/s00338-003-0289-2.

Stuiver M, Polach HA (1977) Discussion. Reporting of ^{14}C Data. *Radiocarbon*. 19:355-63.

Ulm, S (2006) Australian marine reservoir effects: A guide to ΔR values. Australian Archaeology, 63, 57-60

Vargas-Angel B, Thomas JD, Hoke SM (2003) High-latitude *Acropora cervicornis* thickets off Fort Lauderdale, Florida, USA. Coral Reefs 22:464-473

Vollmer SV, Palumbi SR (2007) Restricted gene flow in the Caribbean staghorn coral *Acropora cervicornis*: implications for the recovery of endangered reefs. J Hered. 98:40–50. http://dx.doi.org/10.1093/jhered/esl057

Vollmer SV, Kline DI (2008) Natural Disease Resistance in Threatened Staghorn Corals. Plos ONE, 3(11), 1-5. doi:10.1371/journal.pone.0003718

Wagner AJ (2009) Oxygen and Carbon Isotopes and Coral Growth in the Gulf of Mexico and Caribbean Sea as Environmental and Climate Indicators (Ph.D. thesis). Texas AandM University (p. 64)

Woodley JD (1989) The effects of Hurricane Gilbert on coral reefs at Discovery Bay. In Bacon, P. R. (ed.), Assessment of the Economic Impacts of Hurricane Gilbert on Coastal and Marine Resources in Jamaica. UNEP Regional Seas Rep. Stud. 110, United Nations Environment Programme, Nairobi: 71–73. Rogers, C. S., (1993). Hurricanes and coral reefs: the intermediate disturbance hypothesis revisited. Coral Reefs 12: 127–137

Yates H, Greer L (2016) High Resolution Isotope Sclerochronology Reflects Seasonal Cycle Changes at Rocky Point, Belize between the Last Interglacial and Present. (Unpublished geology undergraduate thesis). Washington and Lee University, Lexington, VA